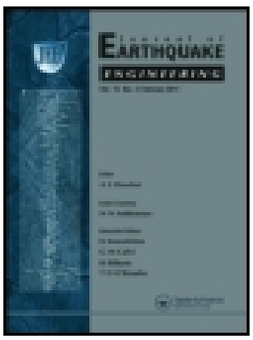

Taylor & Francis
Taylor & Francis Group

Journal of Earthquake Engineering

ISSN: 1363-2469 (Print) 1559-808X (Online) Journal homepage: http://www.tandfonline.com/loi/ueqe20

Improved ASCE/SEI 7-10 Ground-Motion Scaling Procedure for Nonlinear Analysis of Buildings

Juan Carlos Reyes, Catalina González & Erol Kalkan

To cite this article: Juan Carlos Reyes, Catalina González & Erol Kalkan (2018): Improved ASCE/SEI 7-10 Ground-Motion Scaling Procedure for Nonlinear Analysis of Buildings, Journal of Earthquake Engineering, DOI: 10.1080/13632469.2018.1526140

To link to this article: https://doi.org/10.1080/13632469.2018.1526140

Published online: 19 Oct 2018.

JOURNAL OF EARTHQUAKE ENGINEERING
https://doi.org/10.1080/13632469.2018.1526140

Taylor & Francis
Taylor & Francis Group

Improved ASCE/SEI 7-10 Ground-Motion Scaling Procedure for Nonlinear Analysis of Buildings

Juan Carlos Reyes[a], Catalina González[b], and Erol Kalkan [c]

[a]Department of Civil and Environmental Engineering, Universidad de Los Andes, Bogotá, Colombia; [b]Graduate Student, Department of Civil and Environmental Engineering, Universidad de Los Andes, Bogotá, Colombia; [c]Research Structural Engineer, Earthquake Science Center, U. S. Geological Survey, Menlo Park, CA, USA

ABSTRACT

An improved ASCE/SEI 7–10 ground-motion scaling procedure for three-dimensional (3D) response history analysis (RHA) of buildings is presented. In this procedure, different scale factors for two horizontal components of the ground motion are used, and their spectral shapes are considered in ground-motion selection stage. The accuracy of the improved procedure is evaluated by utilizing 3D models of nine asymmetric-plan buildings. It is demonstrated that the improved procedure provides on average 15% conservative estimates of engineering demand parameters while the original version underestimates them on average 29%. Thus, the improved ground-motion selection and scaling procedure is found to be appropriate for nonlinear RHAs of multi-story plan-asymmetric buildings.

ARTICLE HISTORY
Received 23 August 2017
Accepted 16 September 2018

KEYWORDS
Response History Analysis; Dynamic Analysis; Ground-Motion Scaling; Asymmetric-Plan Building; Performance-Based Design; Plan Irregularity

1. Introduction

In seismic performance assessment and design verification of complex structural systems including highly asymmetric-plan buildings, base-isolated systems, and high-rise structures, nonlinear response history analysis (RHA) is a common tool to determine engineering demand parameters (EDPs) for validation of targeted performance criteria. The accurate and efficient estimation of seismic demands using nonlinear RHA relies on proper selection and scaling of ground-motion records. Due to limited number of records available from near-field of earthquakes, ground-motion scaling gains importance for sites within 20 km of active faults, which are capable of generating magnitude seven or larger earthquakes. Both selection and scaling are equally important processes to preserve compliance of records with the site-specific hazard conditions and to account for the aleatoric variability.

Among many procedures proposed to modify ground-motions, the most widely used approaches are amplitude scaling [a list of procedures is given in Katsanos *et al.*, 2010] and spectrum matching [e.g., Lilhanand and Tseng, 1988; Hancock, 2006; Hancock and Bommer, 2007; Al-Atik and Abrahamson, 2010]. The objective of amplitude scaling procedures is to determine scale factors for a small number of records such that the

CONTACT Juan Carlos Reyes jureyes@uniandes.edu.co Department of Civil and Environmental Engineering, Universidad de Los Andes, Bogotá, Colombia.

Color versions of one or more of the figures in the article can be found online at www.tandfonline.com/ueqe.

scaled records provide an accurate estimate of structural responses. The term "accurate" means that the scaled records should provide geometric or arithmetic mean responses close to the "exact" responses considering large population of records compatible with the site-specific hazard conditions.

For scaling records, various intensity measures have been evaluated to minimize the variability in the prediction of EDPs [Mazza and Labernarda, 2017]. In this study, spectral acceleration ordinates are used as the intensity measure. As it will be demonstrated later, spectral responses and EDPs may be assumed as log-normally distributed. Therefore, it is appropriate to represent the "mean" response by the geometric mean (or median), instead of the arithmetic mean [Jayaram and Baker, 2008]—the arithmetic mean is not ideal due to the skewed nature of the EDP data. For a log-normal distribution of a random variable, the geometric mean ($\hat{\mu}$) and median (x_{50}) are given by the same equation: $x_{50} = \hat{\mu} = e^{\mu}$, where μ is the mean of a log-normal distribution. Therefore, it is not misleading to use median instead of geometric mean. Another alternative to represent "mean" response is the 50th percentile of the data, but this alternative representation may be too crude to be useful in the earthquake engineering field.

Previous research [Reyes and Chopra, 2012] demonstrates that, in general, it will not be possible to achieve most accurate estimates of EDPs if both horizontal components of a given ground-motion record are to be scaled by the same factor. Therefore, two different scale factors for the two components of a record can be an alternative choice. Seismologists may find this unconventional approach to be undesirable because it does not preserve focal mechanism and wave travel path effects, inherent in recorded motions. However, if the goal of any ground-motion scaling procedure is to estimate the EDPs accurately—where the benchmark values are determined from a large set of unscaled records, which obviously preserve all the seismological features then such an approach is justified.

Including spectral shape as a criterion for selecting ground-motions is a recommended practice in the literature [Carballo and Cornell, 1998; Ambraseys *et al.*, 2003; Beyer and Bommer, 2007; Kottke and Rathje, 2008; Haselton *et al.*, 2009; Baker, 2011; Jayaram *et al.*, 2011; Haselton *et al.*, 2012; Kwong and Chopra, 2015]. It is shown that avoiding records with pronounced troughs and peaks in their response spectra lead to more accurate estimates of EDPs [Kalkan and Chopra, 2009; Reyes and Chopra, 2012].

The Chapter 16 of the ASCE/SEI 7–10 (henceforth abbreviated as ASCE 7), adopted by the International Building [International Code Council, 2015] and California Building Code [International Code Council, 2016], has been the current industry standard for design verification of important structures. For sites beyond 5 km (3 miles) of the active fault that controls the seismic hazard, the ASCE 7 states that both components of an earthquake record must be scaled by the same factor, determined to ensure that the average of the square-root-of-sum-of-squares (SRSS) response spectra over all records does not fall below the target spectrum for some period range that depends on the fundamental period of the structure. The ASCE 7 approach has the main advantage of using only response spectra of pre-selected records and fundamental period of the structure. However, it has been demonstrated that this procedure leads to inaccurate estimation of story drift, floor velocities and accelerations, even for structures that respond predominantly in the first-"mode" [Kalkan and Chopra, 2012; O'Donnell *et al.*, 2013;

Reyes and Quintero, 2014; Reyes *et al.*, 2014, 2015]. These issues seem to have three main sources: first, focusing the scaling stage on the SRSS spectra; second, using the same scale factor for both component of the record; and third, not considering spectral shape dispersion at the relevant vibration periods of the structure. To overcome some of the weaknesses of the ASCE 7 procedure, which lead to inaccurate estimation of EDPs, new procedures were proposed; such procedures often require additional structural parameters and are computationally more demanding [Kalkan and Chopra, 2010, 2011, 2012; Buratti *et al.*, 2011; Huang *et al.*, 2011; Reyes and Chopra, 2012; Han and Seok, 2013; Reyes and Quintero, 2014; Reyes *et al.*, 2014, 2015].

With the objective of retaining the conceptual simplicity and computational attractiveness of the current ASCE 7 procedure, this paper presents some improvements on the ASCE 7 scaling procedure by allowing un-identical scale factors for the two horizontal components of the record and considering spectral shape of the records at the relevant vibration periods in the ground-motion selection stage. Based on the results from nine multi-story asymmetric-plan buildings with various plan shapes and heights, it is shown that the improved procedure provides on average 15% conservative estimates of EDPs (such as peak values of story drift ratio and rotation ductility demands in girders) with standard deviation of 0.29, while the original ASCE 7 version underestimates them on average 29% with standard deviation of 0.31. In this study, the as-recorded horizontal components (H1 and H2) of the ground motions were applied along the principal directions (x and y) of the structures, respectively.

It should be also noted that the ASCE/SEI 7–16 [American Society of Civil Engineers, 2016] has been released recently. Although this standard has different requirements for the number of time histories and the ground-motion scaling procedures, the ASCE/SEI 7–10 standard is still in effect in the USA. In addition, the ASCE/SEI 7–10 has already been adapted by many countries around the world, and will still remain in use. Because of these reasons, our proposed changes will remain applicable and appropriate.

2. ASCE/SEI 7–10 Ground-Motion Selection and Scaling Procedure

For ground motions recorded beyond 3 miles (5 km) of the active fault that controls the earthquake hazard, ASCE 7 requires that records should be selected from events with magnitudes, fault distances and source mechanisms consistent with those that govern maximum credible earthquake (MCE) ground motions. Both components of the selected ground motion should be scaled by the same factor, determined to ensure that the average of the SRSS response spectra over all records does not fall below the corresponding ordinate of the target spectrum over the period range $0.2T_1$ to $1.5T_1$, where T_1 is the fundamental period of the structure. The SRSS spectrum is computed for the 5%-damped response spectra for the two horizontal ground-motion components. The design value of an EDP—member forces, member deformations, story drifts, etc.—is taken as the average (arithmetic mean) value of the EDP if at least seven scaled records are used in the analyses, or the maximum value of the EDP, otherwise. Various combinations of scale factors for individual records can satisfy the preceding requirement for the average SRSS response spectrum. To achieve the desirable goal of scaling each record by a factor as close to one as possible, the ASCE 7 procedure was implemented by using the approach described in Appendix-A of Reyes and Chopra [2012]. The records were selected by minimizing the

discrepancy between the scaled spectrum of a record and the target spectrum over the period range from $0.2T_1$ to $1.5T_1$, and then identifying the final set of records as those with spectral acceleration values at T_1 close to the target spectrum. This selection procedure was proposed by Reyes and Kalkan [2012] and is not part of the requirements of the ASCE 7.

3. Improved ASCE/SEI 7–10 Ground-Motion Scaling Procedure

As aforementioned, the original ASCE 7 procedure scales both ground-motion components by the same factor, and does not explicitly consider spectral shape as a selection criterion. This procedure is improved here in two ways: first, different scale factors are allowed for the two horizontal components of the record in scaling stage, and second, spectral shape of the record at the relevant vibration periods is considered in selection stage.

In the proposed procedure, the scale factor for a record is composed of two parts: (a) an individual scale factor SF_1 obtain by minimizing the difference between the target and the response spectra; (b) a group scale factor SF_2 calculated for a full set of records to guarantee that the average response spectrum is above the target spectrum; this factor is unique for all the records within the set. The shape of each individual record is qualified by calculating the norm of the difference between the target and the record response spectra for a range of structural periods, which consider lengthening of vibration periods due to nonlinear deformations. To select the final set of records, a large population of M sets is created from records that have the highest shape rank. From these large number of possible sets, the final set is the one with the lowest discrepancy with the target spectrum at the vibration periods of the structure.

This procedure may be implemented as follows:

(1) Obtain the target pseudo-acceleration spectrum, which is typically a site-specific spectrum developed in accordance with the probabilistic MCE, deterministic MCE and minimum requirements of Chapter 21 of ASCE 7. For this study, the target spectra for two orthogonal horizontal components (i.e., x- and y-components) of the records is defined as $\widehat{\mathbf{A}}_\mathbf{x}$ and $\widehat{\mathbf{A}}_\mathbf{y}$ as vectors of median spectral values [$\hat{A}_x(T)$ and $\hat{A}_y(T)$] over the period range from $0.2T_1$ to $1.5T_1$ (100 equally spaced periods are chosen). Here, the components x and y correspond to the as-recorded H1 and H2 components of the records, respectively.
(2) Select a set of k records appropriate for the site, based on the selection criteria specified in ASCE 7. In this study, $k = 7$ following Reyes and Kalkan [2011, 2012].
(3) For the x and y horizontal components of the record, calculate the 5%-damped response spectra $A_x(T)$ and $A_y(T)$, and the vectors $\mathbf{A}_\mathbf{x}$ and $\mathbf{A}_\mathbf{y}$ of spectral values at periods T_i (same as in Step 1).
(4) For each record, determine the scale factors SF_{1x} and SF_{1y} that minimize the difference between the target spectrum (Step 1) and the response spectra (Step 3) for the two horizontal components of the record by solving the following minimization problem:

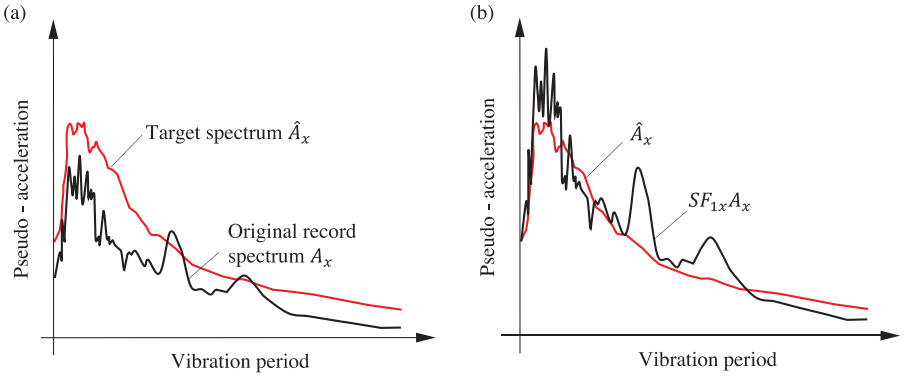

Figure 1. (a) Target pseudo-acceleration spectrum $\widehat{\mathbf{A}}_x$ and individual "unscaled" ground-motion pseudo-acceleration spectrum $\mathbf{A}_x$. (b) Target pseudo-acceleration spectrum $\widehat{\mathbf{A}}_x$ and scaled ground-motion pseudo-acceleration spectrum $SF_{1x}A_x$.

$$SF_{1x} = \min\left\|\widehat{\mathbf{A}}_x - SF_{1x} \cdot \mathbf{A}_x\right\|, SF_{1y} = \min\left\|\widehat{\mathbf{A}}_y - SF_{1y} \cdot \mathbf{A}_y\right\|, \tag{1}$$

This minimization, based on the Euclidean norm, ensures that the scaled response spectrum is as close as possible to the target spectrum, as shown in Fig. 1.

(5) Select the $k + z$ records with the lowest values of $\left\|\widehat{\mathbf{A}}_x - SF_{1x} \cdot \mathbf{A}_x\right\| + \left\|\widehat{\mathbf{A}}_y - SF_{1y} \cdot \mathbf{A}_y\right\|$. These records will be those whose spectra best fit the target spectrum between $0.2T_1$ and $1.5T_1$. Note: It was found that $z = 3$ yields a sufficient number of records to generate the final set; however, larger values may be considered.
(6) Establish all the possible M sets of k records:

$$M = \frac{(k+z)!}{z!k!} \tag{2}$$

This equation corresponds to the number of possible combinations of k different records from a collection of $k + z$ records. Equation (2) is actually the classical combination formula $C(n, r) = n!/(r!(n - r)!)$ adapted for the variables of this case. In this study, M is equal to 120 because we selected $k = 7$ and $z = 3$. For each set, implement steps 7–10.

(7) Determine A_{mx} and A_{my}, defined as the median value of $SF_{1x}A_x$ and $SF_{1y}A_y$, respectively.
(8) Calculate the maximum normalized difference ε_x and ε_y:

$$\varepsilon_x = \max_{0.2T_1 \le T_i \le 1.5T_1}\left(\frac{\hat{A}_{x,i} - A_{mx,i}}{\hat{A}_{x,i}}\right), \varepsilon_y = \max_{0.2T_1 \le T_i \le 1.5T_1}\left(\frac{\hat{A}_{y,i} - A_{my,i}}{\hat{A}_{y,i}}\right), \tag{3}$$

where $\hat{A}_{x,i}$ and $\hat{A}_{y,i}$ are the target pseudo-acceleration spectra at vibration period T_i. Determine the scale factors SF_{2x} and SF_{2y}:

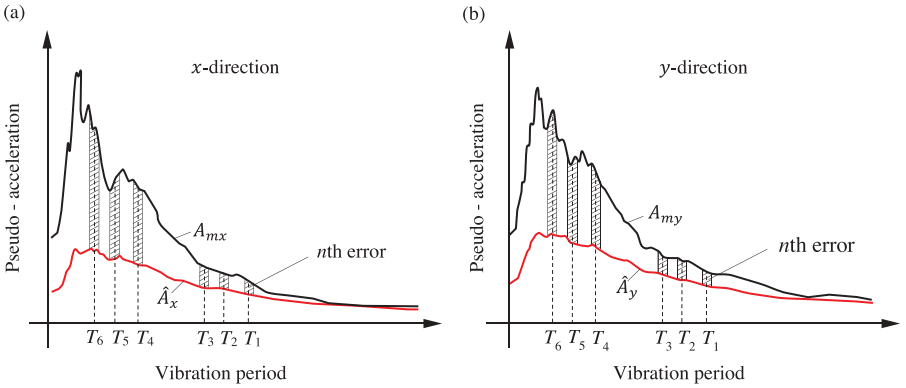

Figure 2. (a) Target pseudo-acceleration spectrum $\hat{A}_x$ and median value of $SF_{1x}A_x$ (A_{mx}). (b) Target pseudo-acceleration spectrum $\hat{A}_y$ and median value of $SF_{1y}A_y$ (A_{my}).

$$SF_{2x} = \frac{1}{1-\varepsilon_x}, \; SF_{2y} = \frac{1}{1-\varepsilon_y}, \tag{4}$$

(9) Determine the final scale factor for each record:

$$SF_x = SF_{1x} \cdot SF_{2x}, \; SF_y = SF_{1y} \cdot SF_{2y}, \tag{5}$$

(10) Calculate the error (Fig. 2):

$$\text{Error} = \sum_{n=1}^{N} \int_{0.9T_n}^{1.1T_n} \left|\hat{A}_x(T) - SF_x A_{mx}(T)\right| dT + \int_{0.9T_n}^{1.1T_n} \left|\hat{A}_y(T) - SF_y A_{my}(T)\right| dT \tag{6}$$

where N is the total number of vibration modes considered (in this study, $N = 6$) and $|.|$ is the absolute value. We use $N = 6$ (two triplets of modes) to consider at least the first and second modes with the largest effective modal mass in each direction. The integration limits were selected within 10% margin to minimize the effect of high variations of response spectra near the selected periods. Recall that period elongation was already considered in Step 1 by using a period range from $0.2T_1$ to $1.5T_1$. Steps 7 through 10 are implemented for each of the M sets.

(11) Select the final set of records as the set with the lowest Error value.

4. Structural Systems

Three different building types with various plans and number of stories were used for testing the original and improved ASCE 7 ground-motion scaling procedures. These structures are identified by letters "R", "L," and "T". Plan R stands for quasi-rectangular, plan T is symmetric about y-axis, and plan L is asymmetric about both x- and y-axes. The

Table 1. Fundamental periods of buildings (i.e., periods with the largest mass participation in each horizontal direction).

Building ID	R05	R10	R15	L05	L10	L15	T05	T10	T15
Fundamental period in *x*-dir, s	0.85	1.05	1.49	0.64	1.29	1.83	0.52	1.23	1.59
Fundamental period in *y*-dir, s	1.03	1.53	2.51	0.64	1.21	1.70	0.63	1.23	1.93

number of stories follows the letters R, L, and T. For example, "R05" indicates a five-story rectangular plan building. The structures considered are nine multi-story buildings with 5, 10, and 15 stories. Their fundamental periods are presented in Table 1. These hypothetical buildings were designed to be located in Los Angeles, California according to the 2010 California Building Code [International Code Council, 2010]. The lateral resisting system of the buildings consists of moment-resisting frames. Their plan shapes are shown in Fig. 3 where the moment resisting frames (MRFs) are highlighted. The buildings have similar plan areas and floor weights, with a span length of 30 ft (9.14 m) and a story height of 10 ft (3.05 m). The earthquake design forces were determined by bi-directional linear response spectrum analysis of each building with the design spectrum reduced by a response modification factor $R_y = 8$. However, most member sizes were governed by drift limits instead of strength requirements.

To verify that the selected buildings cover a broad range of torsional irregularities, the following irregularity factor (β) was calculated for each building per ASCE 7:

$$\beta = {}^{\Delta_{\max}}/_{\Delta_{\text{average}}} \tag{7}$$

where $\Delta_{\max}$ is the maximum story drift and Δ_{average} is the average story drift at the two ends of the structure. The level of torsional irregularity is classified according to the ASCE 7 standard:

- no torsional irregularity: $\beta < 1.2$,
- torsional irregularity: $1.2 \leq \beta \leq 1.4$ and,
- extreme torsional irregularity: $\beta > 1.4$.

The buildings cover these three levels of torsional irregularity as demonstrated in Table 2, where the values of β are shown in ascending order. To estimate β, conventional linear response spectrum analysis was conducted for each building; $\Delta_{\max}$ was calculated as the maximum drift at the corners (over all stories) in each principal direction (x or y); Δ_{average} was obtained as the average story drift at the two ends of the story in which $\Delta_{\max}$ took place. β was calculated for each orthogonal direction and its maximum value was reported in Table 2. The final plan layout of MRFs of the buildings was influenced not only by the level of torsional irregularity but also by the structural periods. Due to the shape of the design spectrum, the design accelerations of mid-rise buildings were smaller than those of the low-rise buildings; this affected directly internal forces and story drifts. For the research purpose, it was also desirable to achieve different irregularity factors β between the structures. These aspects led, for example, to include an additional internal frame for structure R10, that was not present in building R15; however, member sizes of the building R15 were much heavier than those of the building R10.

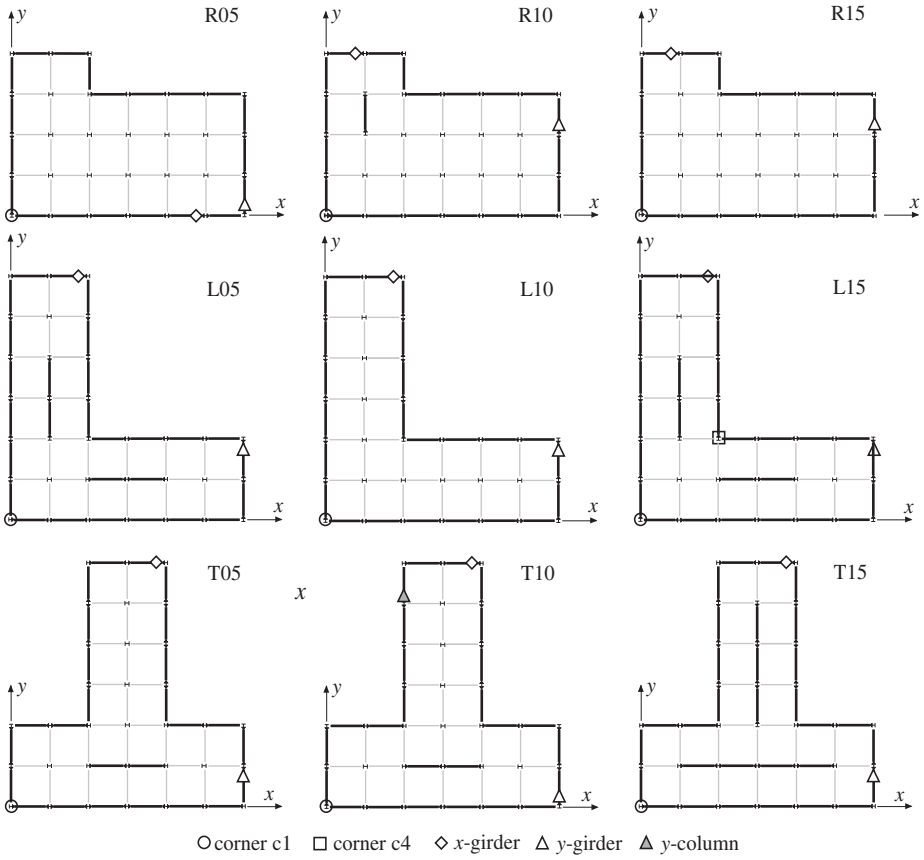

Figure 3. Plan views of nine asymmetric plan buildings. Marked corners and girders are selected purposely to measure maximum engineering demand parameters. Plan R stands for quasi-rectangular; plan T is symmetric about *y*-axis, and plan L is asymmetric about both *x*- and *y*-axes. Letters R, L, and T are followed by the number of stories; for example, R05 indicates a five-story rectangular plan building.

Table 2. Torsional irregularity factors.

Building ID	R05	R15	R10	L10	L15	T15	L05	T10	T05
β	1.00	1.10	1.13	1.20	1.26	1.30	1.35	1.41	1.43

Figure 4, showing the effective modal masses of the buildings, permits the following observations: (a) lateral displacements dominate motion of the R-plan and L10 buildings in the first and second modes, whereas torsion controls motion in the third mode, indicating weak coupling between lateral and torsional components of motion; (b) coupled lateral-torsional motions occur in the first and third mode of L05, T05, and T10 buildings whereas lateral displacements dominate motion in the second mode; and (c) lateral displacement controls motion in the first mode, whereas coupled lateral-torsional motions occur in the second and third mode of T15 plan. It is expected that the contribution of higher modes be important in the selection and scaling of records, especially in structures where the effective mass of the fundamental mode is low. Note that these conclusions are drawn from linear analyses, and nonlinear behavior may

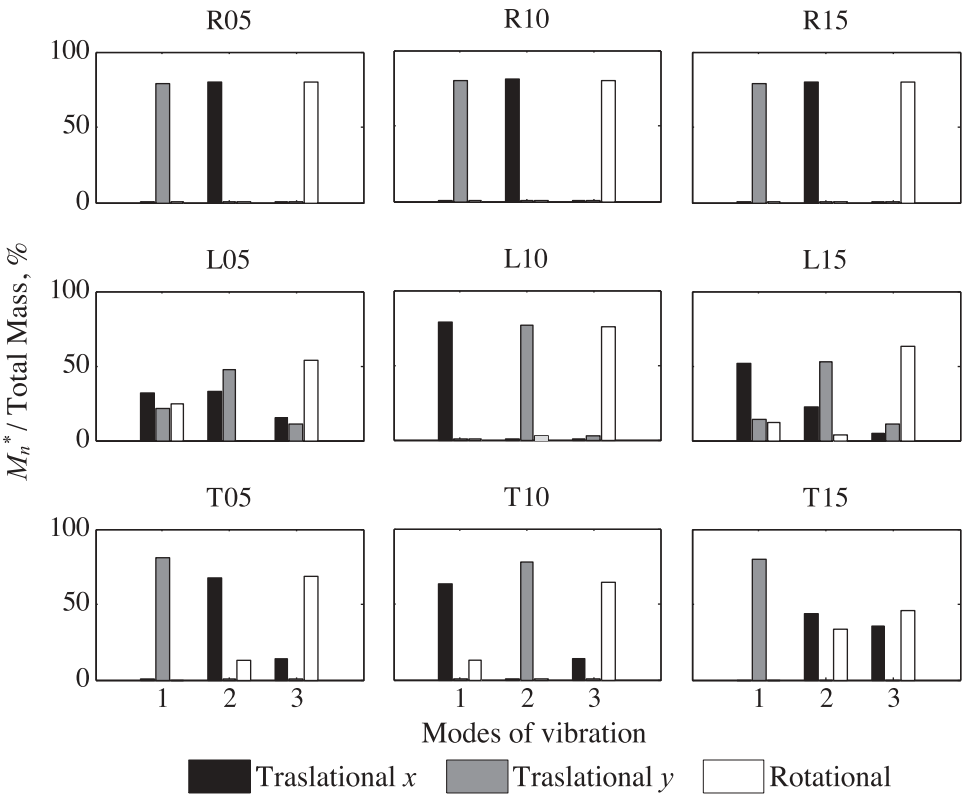

Figure 4. Ratios of effective modal masses M_n^* to total masses in translational x, y and rotational directions for 5-, 10-, and 15-story buildings with three different floor plans.

diminish or escalate the lateral torsional motions of the buildings. Further details of the structural systems including their fundamental periods, mode shapes, torsional irregularity factors, etc. can be found in Reyes *et al.* [2014].

Nonlinear RHAs of the buildings were conducted using PERFORM-3D [Computers and Structures Inc, 2006]. The following features were used in the finite element modeling:

- Girders were modeled by a linear element with tri-linear plastic hinges at the ends of the elements that can include intra-cycle strength deterioration, but not cyclic stiffness degradation; back-bone curves and strength deterioration rules were taken from the ASCE/SEI 41–13 [American Society of Civil Engineers, 2014] with modification on the descending branch of the backbone curve to achieve convergence. In PERFORM-3D, each girder element has the following components: (a) two rigid end-zones, (b) two rigid-plastic moment hinges (rotation type), and (c) one linear beam element with a standard steel section.
- Columns were modeled by using a lumped plasticity model conformed by a linear element with two tri-linear plastic hinges at its ends. Axial load-moment (P-M-M) interaction was based on the plasticity theory. XTRACT software [Chadwell and Imbsen, 2004] was used to obtain the capacities and the P-M-M yield surface

parameters of the elements. The plastic hinges include intra-cycle strength deterioration but not cyclic stiffness degradation. In PERFORM-3D, each column element has the following components: (a) two rigid end-zones, (b) two rigid-plastic P-M-M hinges (rotation type), and (c) one linear column element with a standard steel section. Ductility capacities and backbones of the plastic hinges were specified according to the ASCE/SEI 41–13. Columns of MRFs were assumed to be fixed at the base, whereas gravity columns were considered pinned.

- Panel zones were modeled as four rigid links hinged at the corners with a rotational spring that represents the strength and stiffness of the connection; strength and stiffness properties of the panel zones were obtained from the formulations proposed by Krawinkler [1978]. In PERFORM-3D, this element is called"panel zone component."
- Effects of nonlinear geometry were approximated by a standard P-Δ formulation for both moment and gravity frames.
- Floor diaphragms were assumed to be rigid. In PERFORM-3D, this is done by defining horizontal rigid diaphragms that constrain the horizontal and rotational displacements of all the nodes of each floor.

5. Ground-Motion Ensemble

The 30 ground-motion records selected for this investigation were obtained from the University of California, Berkeley Pacific Earthquake Engineering Research Center Ground-Motion Database (see "Data and Resources"). The ground motions listed in Table 3 were used without rotating them to their maximum directions. In order to account for the aleatoric uncertainty, we avoided selection of 30 records from the same event, and these records were recorded from seven shallow crustal earthquakes with moment magnitude between 6.5 and 6.9 at closest distances (R_{JB}) ranging from 19.8 to 29.5 km, and with NEHRP site classification C (very dense soil or soft rock) or D (stiff soil)—compatible with typical seismic hazard conditions in Los Angeles.

Because these ground motions were not intense enough to drive the buildings far into the inelastic range—an obvious requirement to fully test any ground-motion scaling procedure—they were pre-amplified by a factor of four. This factor was selected based on some preliminary analyses that show low nonlinear incursions of the buildings for at least 50% of the original records. The pre-amplified ground motions are treated as "unscaled" records without rotating them to any principal directions. This evaluation approach has been previously used in Kalkan and Chopra [2012], Reyes and Chopra [2012], and Reyes and Quintero [2014, 2015]. Shown in Fig. 5 are the 5%-damped median response spectra for x- and y-components of the original records. The median spectra of x- and y-components of ground motions are taken as the target spectra in two orthogonal directions for purposes of evaluating the improved ASCE 7 procedure.

It should be noted that our objective was to create a sample of records from a representative subset of a population of already recorded ground motions under similar magnitude, distance, and site conditions. The best way to avoid a biased or unrepresentative sample is to use simple random sampling, which is a fair way of selecting a sample

Table 3. List of 30 ground-motion records.

GM ID	Earthquake name	Date M/D/Y	Station name	M_w	R_{JB}km	PGA *x*-dir., *g*	PGA *y*-dir., *g*	NEHRP site class
1	San Fernando, CA	02/09/1971	LA – Hollywood Stor FF	6.6	22.8	0.21	0.17	D
2	San Fernando, CA	02/09/1971	Santa Felita Dam (Outlet)	6.6	24.7	0.10	0.18	C
3	Imperial Valley-06, CA	10/15/1979	Calipatria Fire Station	6.5	23.2	0.77	0.13	D
4	Imperial Valley-06, CA	10/15/1979	Delta	6.5	22.0	0.32	0.24	D
5	Imperial Valley-06, CA	10/15/1979	El Centro Array #1	6.5	19.8	0.14	0.14	D
6	Imperial Valley-06, CA	10/15/1979	El Centro Array #13	6.5	22.0	0.12	0.14	D
7	Imperial Valley-06, CA	10/15/1979	Superstition Mtn Camera	6.5	24.6	0.20	0.10	C
8	Irpinia, Italy-01	11/23/1980	Brienza	6.9	22.5	0.21	0.21	C
9	Superstition Hills-02, CA	11/24/1987	Wildlife Liquef. Array	6.5	23.9	0.19	0.21	D
10	Loma Prieta, CA	10/18/1989	Agnews State Hospital	6.9	24.3	0.14	0.17	D
11	Loma Prieta, CA	10/18/1989	Anderson Dam (Downstream)	6.9	19.9	0.20	0.27	C
12	Loma Prieta, CA	10/18/1989	Anderson Dam (L Abut)	6.9	19.9	0.07	0.06	C
13	Loma Prieta, CA	10/18/1989	Coyote Lake Dam (Downst)	6.9	20.4	0.19	0.16	D
14	Loma Prieta, CA	10/18/1989	Coyote Lake Dam (SW Abut)	6.9	20.0	0.45	0.18	C
15	Loma Prieta, CA	10/18/1989	Gilroy Array #7	6.9	22.4	0.32	0.27	D
16	Loma Prieta, CA	10/18/1989	Hollister – SAGO Vault	6.9	29.5	0.05	0.05	C
17	Northridge, CA	01/17/1994	Castaic – Old Ridge Route	6.7	20.1	0.53	0.49	C
18	Northridge, CA	01/17/1994	Glendale – Las Palmas	6.7	21.6	0.23	0.28	C
19	Northridge, CA	01/17/1994	LA – Baldwin Hills	6.7	23.5	0.26	0.19	D
20	Northridge, CA	01/17/1994	LA – Centinela St	6.7	20.4	0.42	0.28	D
21	Northridge, CA	01/17/1994	LA – Cypress Ave	6.7	29.0	0.17	0.23	C
22	Northridge, CA	01/17/1994	LA – Fletcher Dr	6.7	25.7	0.19	0.28	C
23	Northridge, CA	01/17/1994	LA – N Westmoreland	6.7	23.4	0.34	0.32	D
24	Northridge, CA	01/17/1994	LA – Pico & Sentous	6.7	27.8	0.12	0.19	D
25	Kobe, Japan	01/16/1995	Abeno	6.9	24.9	0.20	0.16	D
26	Kobe, Japan	01/16/1995	Kakogawa	6.9	22.5	0.36	0.18	D
27	Kobe, Japan	01/16/1995	Morigawachi	6.9	24.8	0.19	0.16	D
28	Kobe, Japan	01/16/1995	OSAJ	6.9	21.4	0.08	0.07	D
29	Kobe, Japan	01/16/1995	Sakai	6.9	28.1	0.14	0.16	D
30	Kobe, Japan	01/16/1995	Yae	6.9	27.8	0.15	0.14	D

GM ID: ground-motion identification number; M_w = moment magnitude; R_{JB} = Joyner–Boore distance; PGA = peak ground acceleration; NEHRP: National Earthquake Hazard Reduction Program.

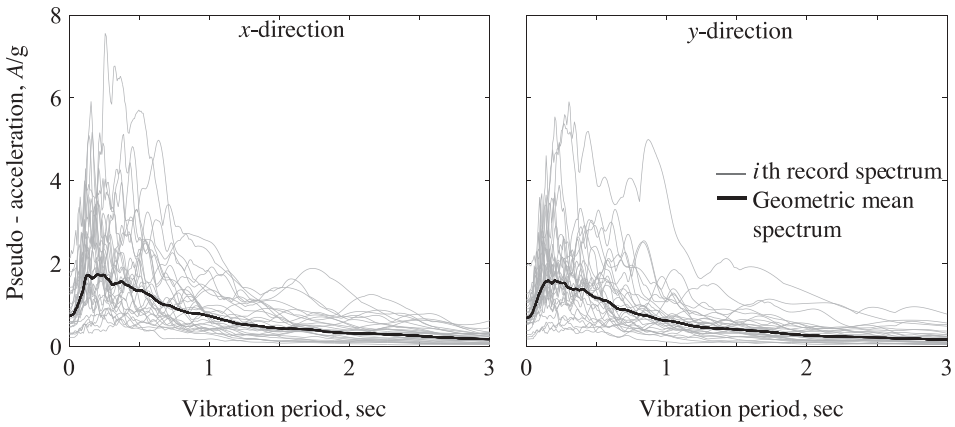

Figure 5. Geometric-mean pseudo-acceleration response spectra of 30 original records in two orthogonal directions for 5% damping; individual response spectra of the records are also shown.

from a given population since every ground-motion is given equal opportunity of being selected; thus, selection of 30 records from the representative subset of the population was conducted randomly [Davison, 2009]. This process statistically allows us to treat the median spectrum of this random sample as the "true" target spectrum.

The structures were subjected to sets of seven records scaled according to the original and improved ASCE 7 procedures, and their responses were compared against the benchmark values, defined as the median values of the EDPs obtained from nonlinear RHAs of the structure subjected to 30 "unscaled" records. These selected seven records are from multiple events, and their spectral shapes show significant aleatoric variability. For example, the acceleration response spectra of ground motions selected for L05 building for the x and y horizontal components are shown in Figs. 6 and 7, respectively. These figures illustrate how the spectral shapes of the selected records match with each other once they are modified by the scale factors developed by the improved procedure. The scale factors used for the L05 building and the other buildings in these figures are listed in Table 4. It should be noted that the ground motions were applied along the principal directions of the structures per ASCE 7.

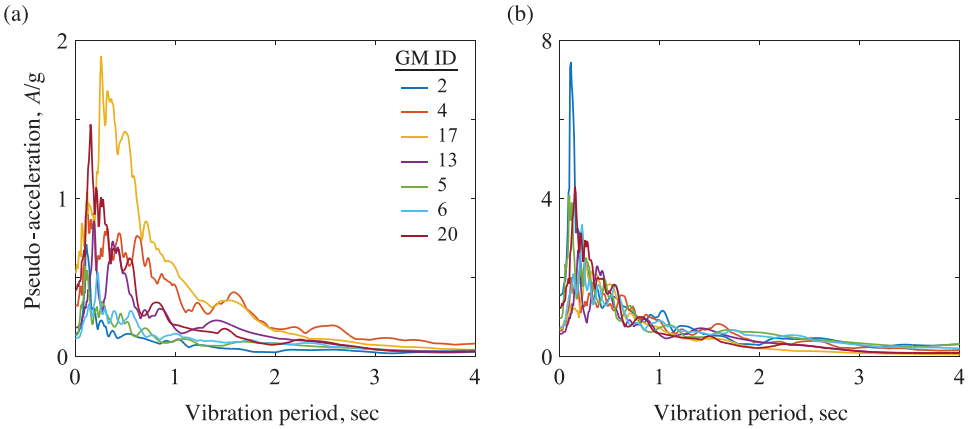

Figure 6. (a) Ground-motion response spectra A_x of the selected set of records for building L05 in the x-direction. (b) Scaled ground-motion response spectra SF_xA_x of the selected set of records for building L05 in the x-direction.

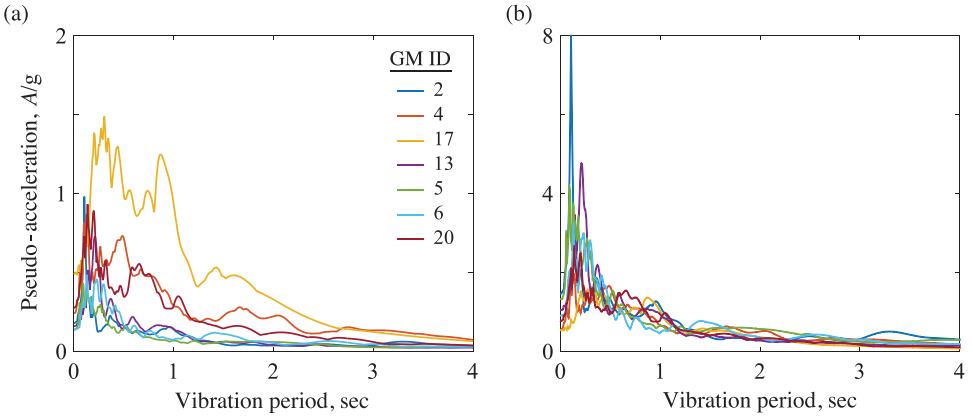

Figure 7. (a) Ground-motion response spectra A_y of the selected set of records for building L05 in the y-direction. (b) Scaled ground-motion response spectra SF_yA_y of the selected set of records for building L05 in the y-direction.

Table 4. Ground-motion scale factors from the improved ASCE 7 procedure.

Building ID								
R05	GM ID	*29*	*26*	*17*	*2*	*4*	*19*	*10*
	SF_x	4.93	2.18	1.30	10.29	2.25	3.93	5.40
	SF_y	4.15	4.07	1.15	8.47	2.51	4.03	3.74
R10	GM ID	*2*	*4*	*17*	*13*	*5*	*6*	*20*
	SF_x	10.44	2.04	1.29	3.15	7.10	6.27	2.91
	SF_y	8.19	2.28	1.09	6.55	9.45	6.41	2.79
R15	GM ID	*4*	*8*	*30*	*17*	*2*	*19*	*24*
	SF_x	1.84	7.87	2.21	1.38	9.17	4.08	5.23
	SF_y	2.06	5.74	2.24	1.01	7.04	3.46	4.08
L05	GM ID	*26*	*25*	*4*	*29*	*9*	*11*	*3*
	SF_x	2.18	4.49	2.35	5.15	3.25	3.33	10.17
	SF_y	4.17	4.77	2.42	4.07	3.29	2.10	6.36
L10	GM ID	*17*	*4*	*2*	*29*	*6*	*19*	*3*
	SF_x	1.25	2.08	10.23	4.85	6.38	3.82	9.05
	SF_y	1.16	2.46	8.73	4.28	6.43	3.90	7.19
L15	GM ID	*4*	*2*	*17*	*13*	*20*	*5*	*24*
	SF_x	1.95	9.90	1.30	3.06	2.97	6.81	5.64
	SF_y	2.24	8.07	1.10	6.65	2.78	9.65	4.28
T05	GM ID	*26*	*25*	*4*	*29*	*9*	*11*	*3*
	SF_x	2.16	4.48	2.33	5.12	3.23	3.29	10.11
	SF_y	4.18	4.77	2.42	4.07	3.30	2.11	6.37
T10	GM ID	*17*	*29*	*4*	*2*	*5*	*6*	*19*
	SF_x	1.26	4.87	2.10	10.24	7.11	6.38	3.83
	SF_y	1.17	4.34	2.50	8.87	9.53	6.44	3.99
T15	GM ID	*4*	*2*	*17*	*13*	*20*	*5*	*24*
	SF_x	1.94	9.83	1.32	3.11	2.98	6.73	5.60
	SF_y	2.22	8.10	1.09	6.78	2.76	9.60	4.28

6. Evaluation Methodology

The improved and original ASCE 7 procedures were evaluated by comparing the median value of an EDP against the benchmark value, defined as the median value of the EDP obtained from nonlinear RHA of the structures subjected to the 30 "unscaled" records (Table 3). The median values of the EDPs were determined by nonlinear RHA of the buildings from a set of seven ground motions, scaled according to the ASCE 7 original and improved procedures. The EDPs selected are peak values of story drift ratio and rotation ductility demands in girders. This evaluation procedure was also used in Kalkan and Chopra [2010, 2011], Kalkan and Kwong [2010, 2012], Reyes and Chopra [2012] and Reyes and Quintero [2014, 2015].

Here, it is assumed that the EDPs are log-normally distributed. Constructing probability distribution plots of various EDPs supported this assumption. Probability distribution is a mathematical function that delivers the likelihoods of occurrence of different possible outcomes within the population. As an example, Fig. 8 shows a probability distribution plot of first-story drift values obtained at the center of mass of the building L15. It is apparent that data are log-normally distributed because they follow a linear trend; therefore, it is appropriate to represent the "mean" response by the geometric mean (or median), instead of the arithmetic mean.

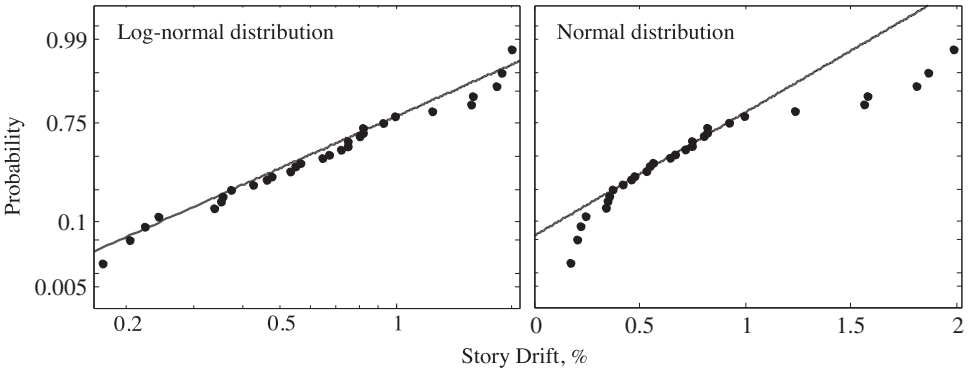

Figure 8. Probability plots of first story drifts at the center of mass of building L15 subjected to 30 "unscaled" ground motions.

7. Results

7.1. *R-Plan Buildings*

For R-plan buildings having 5, 10, and 15 stories, Fig. 9 shows the story drifts (i.e., inter-story drift ratio) at the center of mass (Fig. 3). First, second and third columns of this figure depict the EDP values in x-direction for the benchmark, original ASCE 7 procedure and the improved ASCE 7 procedure, respectively; the next three columns show similar results in y-direction. The markers and horizontal lines represent the median EDP value and 16^{th} and 84^{th} percentile of the EDP assuming a lognormal distribution. For comparison purposes, the median benchmark values are kept in all sub-plots as dashed lines. In order to be consistent with comparisons of the original and improved ASCE 7 procedures, geometric mean was used for the ASCE 7 original version although the ASCE 7 requires arithmetic mean. The use of geometric mean instead of arithmetic mean does not affect the conclusions because geometric mean is consistently used for both scaling methods [Kalkan and Chopra, 2011].

The discrepancies between the benchmark EDPs and EDPs based on the original ASCE 7 and improved ASCE 7 procedures are measured. A negative discrepancy means that the scaling procedure underestimates the actual EDP, and a positive discrepancy implies that the scaling procedure overestimates the response. As demonstrated in Fig. 9, the records scaled according to the improved ASCE 7 procedure provide median values of EDPs that are much closer to the benchmark values than is achieved by the original ASCE 7 procedure; for example, compare columns 2 and 3 of Fig. 9. The maximum underestimation of 31% in story drifts (building R10) by scaling records according to the original ASCE 7 procedure is now conservatively estimated with 19% when these records are scaled by the improved procedure; likewise, the maximum error in buildings R05 and R15 is reduced from −20% to +16% and from −23% to +20%, respectively. Table 5 summarizes the maximum discrepancies in story drifts at the center of mass according to the original and improved ASCE 7 procedures for all buildings.

Rotation ductility demands μ were calculated as $1 + \theta_p/\theta_y$, where θ_p is the plastic rotation and θ_y is the yield rotation as defined in the ASCE/SEI 41–13. Representative

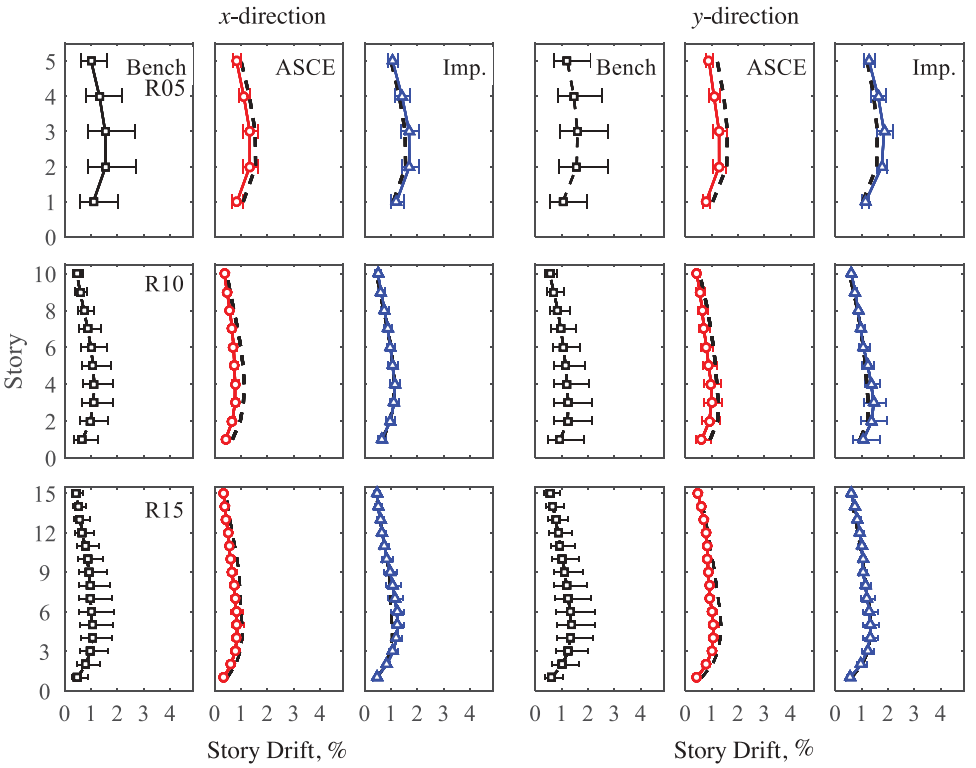

Figure 9. Story drift values in percentage in *x*- and *y*-direction at center of mass for R-plan 5-, 10-, and 15-story buildings. In each panel, the marker represents the median value, and the horizontal bars indicate the 16th and 84th percentile of the EDP assuming a log-normal distribution. "Bench" stands for benchmark, "ASCE" for ASCE 7 scaling procedure, and "Imp." for improved ASCE 7 scaling procedure. Median values of benchmark results are marked in panels showing results of ASCE and Imp. as dashed curves.

Table 5. Maximum discrepancies observed in story drifts at the center of mass; positive values indicate overestimation, and negative values denote underestimation of benchmark story drift values (ASCE 7: ASCE/SEI 7–10 ground-motion scaling procedure; Imp.: improved ASCE 7 ground-motion scaling procedure).

Building ID	ASCE 7 (%)	Imp. (%)
R05	−20	+16
R10	−31	+19
R15	−23	+20
L05	−38	+20
L10	−28	+22
L15	−27	+39
T05	−24	+12
T10	−37	+22
T15	−22	+22

results for rotation ductility demands in girders for building R05, R10, and R15 are shown in Fig. 10; the selected girders are highlighted in Fig. 3 by diamond and triangle markers. The markers in Fig. 10 represent the median value of the μ and the horizontal bars denote the interval of μ between the first and the third quartile of the data because we found that

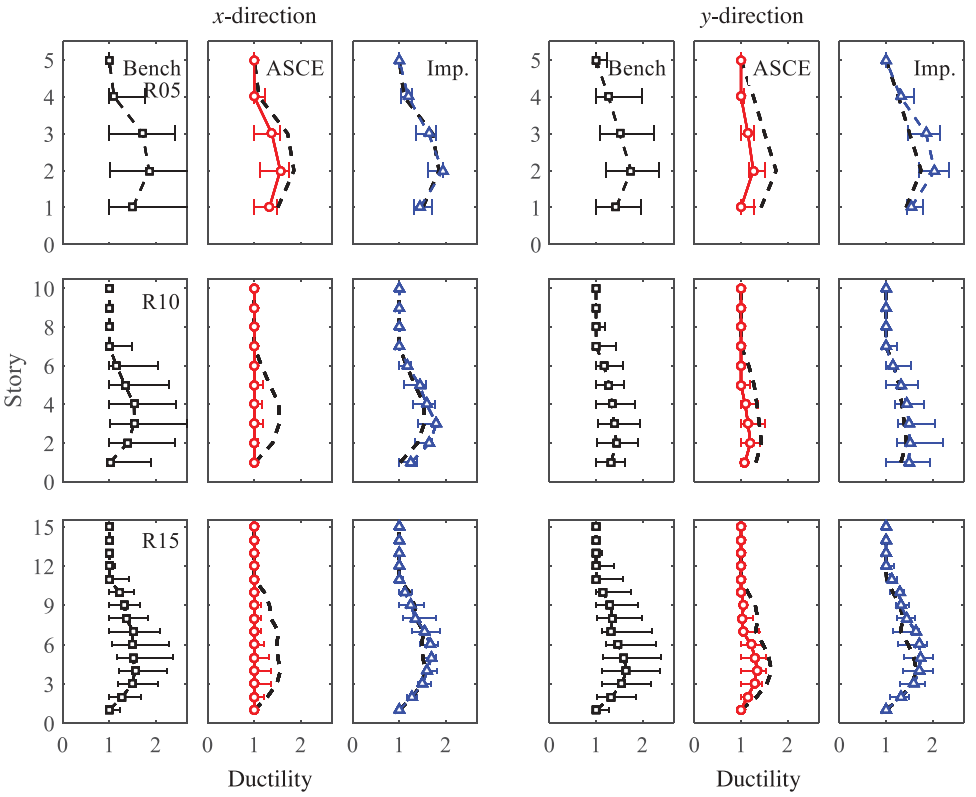

Figure 10. Ductility demands in *x*- and *y*-direction are shown for R-plan 5-, 10-, and 15-story buildings. In each panel, the marker represents the median value, and the horizontal bars indicate the interval of ductility demand values between the first and the third quartile of the data. "Bench" stands for benchmark, "ASCE" for ASCE 7 scaling procedure, and "Imp." for improved ASCE 7 scaling procedure. Median values of benchmark results are marked in panels showing results of ASCE and Imp. as dashed curves.

μ is not log-normally distributed. It is evident that maximum discrepancies encountered by scaling records according to the original ASCE 7 procedure are reduced when these records are scaled by the improved procedure. These results indicate that the original ASCE 7 scaling procedure tends to underestimate the ductility demands by 25% to 36% in most cases. For building R10, the maximum discrepancy of −34% in ductility demands observed by scaling records according to the original ASCE 7 procedure, is modified to +21% when these records are scaled by the improved ASCE 7 procedure; likewise, the maximum discrepancy in building R15 is reduced from −36% to +12%.

The record-to-record variability is not much less in EDPs due to a set of records scaled by the improved ASCE 7 procedure compared to the records scaled by the original procedure because the original ASCE 7 procedure was implemented using an algorithm that already considered spectral shape in the selection stage [Reyes and Chopra, 2012]. These results show that EDPs obtained from ground-motion sets selected and scaled according to the proposed methodology represent a considerable improvement in accuracy when compared to EDPs obtained from the sets scaled according to the ASCE 7

procedure. The ASCE 7 original procedure leads to large underestimations while the improved ASCE 7 leads to conservative results for those structures without torsional irregularities $\beta <$ 1.2.

7.2. *L-Plan Buildings*

For the L-plan buildings (1.2 $\leq \beta \leq$ 1.4), the records scaled according to the improved ASCE 7 procedure resulted in more accurate estimates of median EDP values than the original ASCE 7 procedure. For example, the building L05, which has the highest level of torsional irregularity ($\beta =$ 1.35) for this plan type, presents the maximum enhancement in terms of story drifts estimations (Table 5): from −38% with the ASCE 7 original procedure to +20% for the improved procedure. This enhancement in accuracy is demonstrated in Fig. 11 where the story drifts at the center of mass (Fig. 3) from the records scaled and selected according to the original and improved procedures are shown together with the benchmark EDP values. The original procedure resulted in errors above −27% in most cases, and up to 38% underestimation of story drifts for the building L05 (Table 5).

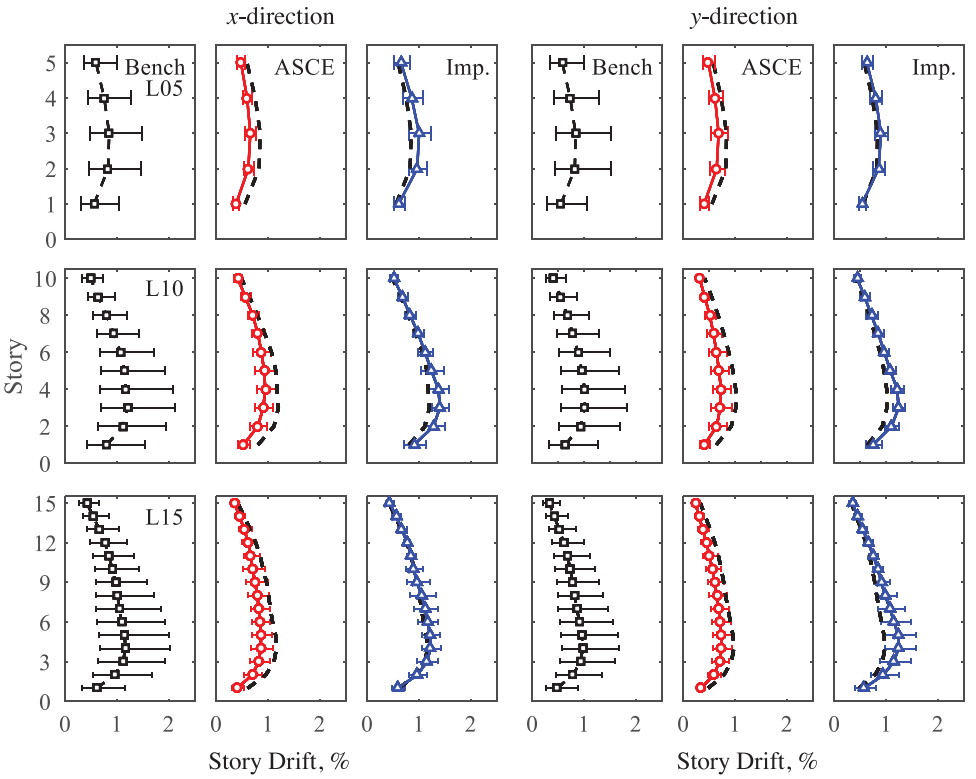

Figure 11. Story drift values in percentage in *x*- and *y*-direction at center of mass for L-plan 5-, 10-, and 15-story buildings. In each panel, the marker represents the median value, and the horizontal bars indicate the 16th and 84th percentile of the EDP assuming a log-normal distribution. "Bench" stands for benchmark, "ASCE" for ASCE 7 scaling procedure, and "Imp." for improved ASCE 7 scaling procedure. Median values of benchmark results are marked in panels showing results of ASCE and Imp. as dashed curves.

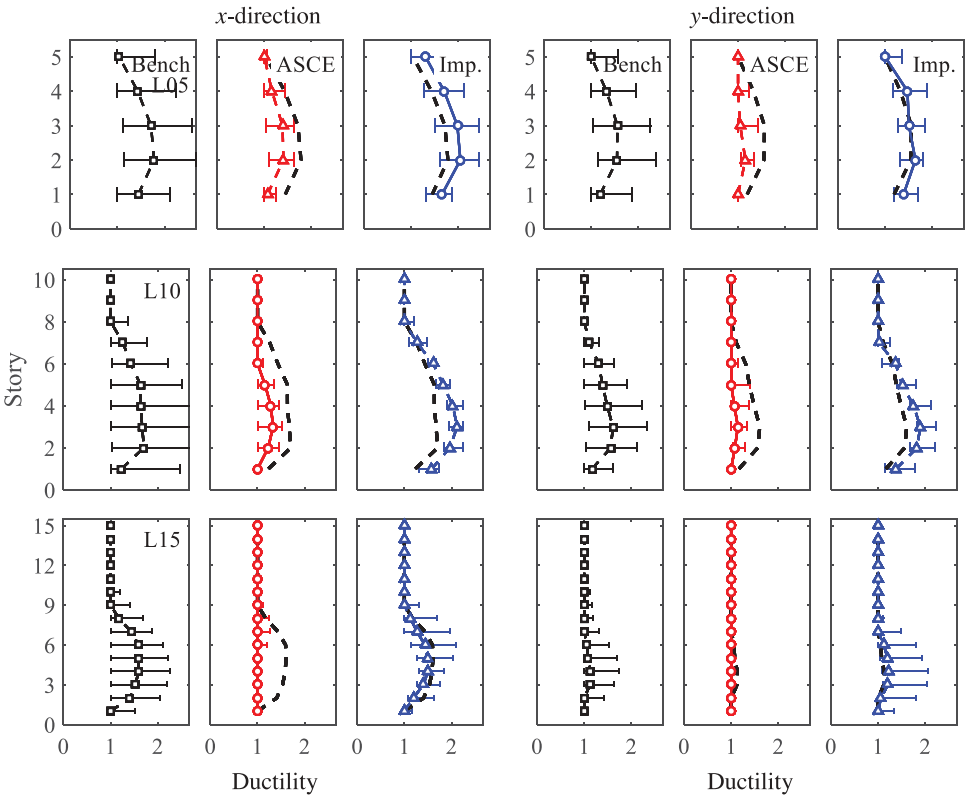

Figure 12. Ductility demands in *x*- and *y*-direction are shown for L-plan 5-, 10-, and 15-story buildings. In each panel, the marker represents the median value, and the horizontal bars indicate the interval of ductility demand values between the first and the third quartile of the data. "Bench" stands for benchmark, "ASCE" for ASCE 7 scaling procedure, and "Imp." for improved ASCE 7 scaling procedure. Median values of benchmark results are marked in panels showing results of ASCE and Imp. as dashed curves.

In contrast, the improved procedure yielded conservative estimates of EDPs; for example, the error in story drifts decreases from −38% to +20% for the building L05 and from −28% to +22% for the building L10. As shown in Fig. 12, the original ASCE 7 procedure underestimated ductility demands in the order of 30–44%, while the improved procedure overestimated them in the range of 18–28% in most cases.

7.3. *T-Plan Buildings*

Similar to the results of the buildings with R- and L-plan, the EDPs obtained from ground-motion sets scaled according to the original procedure are less accurate than those obtained from the improved procedure. The original ASCE 7 procedure generally underestimates the story drifts at lower stories. In contrast, the improved procedure provides more accurate estimates of story drifts, and leads to more conservative results; for example, compare columns 5 and 6 of Fig. 13. Even for T-plan structures with extreme torsional irregularities ($\beta > 1.4$), the proposed procedure becomes conservative. For

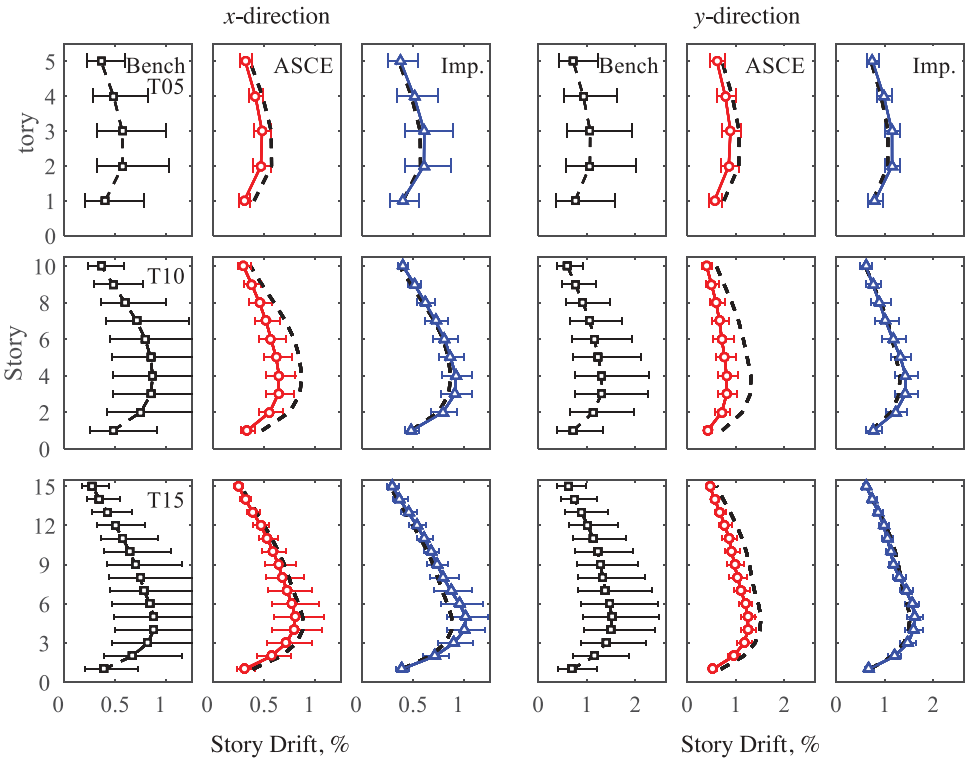

Figure 13. Story drift values in percentage in *x*- and *y*-direction at corner for T-plan 5-, 10-, and 15-story buildings. In each panel, the marker represents the median value, and the horizontal bars indicate the 16th and 84th percentile of the EDP assuming a log-normal distribution. "Bench" stands for benchmark, "ASCE" for ASCE 7 scaling procedure, and "Imp." for improved ASCE 7 scaling procedure. Median values of benchmark results are marked in panels showing results of ASCE and Imp. as dashed curves.

instance, compare columns 5 and 6 of Fig. 13 for the building T10. For this building the maximum discrepancy of −37% in story drifts is reduced to around +22% when the records are scaled by the improved procedure (Table 5). Figure 14 shows the ductility demands for T05, T10, and T15 buildings. For the building T15, the underestimation of 41% in ductility demands from the original procedure is reduced to 18% when the improved procedure is implemented. The T05 ($\beta = 1.43$) and T10 ($\beta = 1.41$) buildings present improvements in story drifts that varies from −24% to +12% and from −37% to +22% (Table 5), showing that the improved procedure leads to more conservative results even when the torsional irregularity increases.

8. Conclusions

In this study, the ASCE/SEI 7–10 [ASCE 7: American Society of Civil Engineers, 2010] ground-motion scaling procedure is modified by determining scale factors for two components of the ground motions to be used in three-dimensional response history analyses of buildings with various degrees of plan asymmetry. The accuracy of the improved procedure was evaluated against the original ASCE 7 procedure by comparing the median values of the EDPs from a set of seven records scaled according to both procedures against

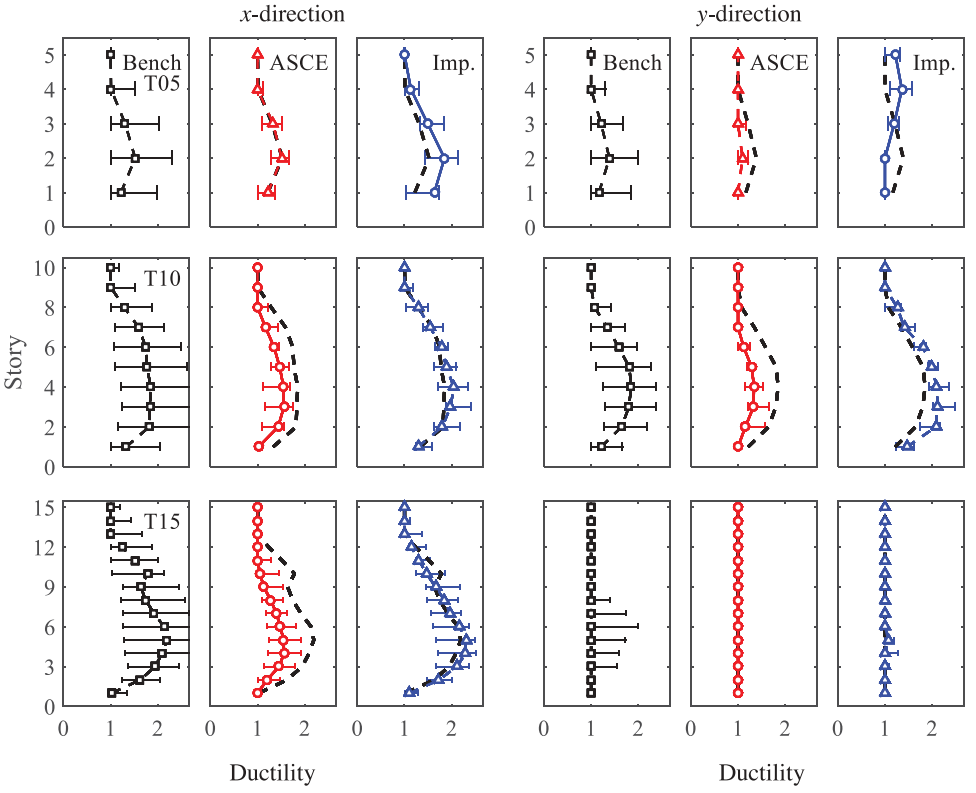

Figure 14. Ductility demands in *x*- and *y*-direction are shown for T-plan 5-, 10-, and 15-story buildings. In each panel, the marker represents the median value, and the horizontal bars indicate the interval of ductility demand values between the first and the third quartile of the data. "Bench" stands for benchmark, "ASCE" for ASCE 7 scaling procedure, and "Imp." for improved ASCE 7 scaling procedure. Median values of benchmark results are marked in panels showing results of ASCE and Imp. as dashed curves.

the benchmark values. A suite of nine multi-story asymmetric-plan buildings was used for testing. For each building, a different set of seven records was used because the improved procedure considers spectral shape of the records at the relevant vibration periods of the building in the ground-motion selection stage. This evaluation led to the following conclusions:

(1) The ASCE 7 original procedure provides inaccurate estimates of the median EDPs in one or both horizontal directions, leading to underestimations of story drift and rotation ductility demands in all cases (a total of nine cases for each EDP). In contrast, the improved procedure provides conservative results, and preserves the conceptual simplicity and practicality of the original ASCE 7 procedure. The improved procedure provides on average 15% conservative estimates of EDPs while the original version underestimates them on average 29% for all buildings considered.
(2) In the original ASCE 7 procedure, the scaling is performed considering the SRSS spectrum that summarizes the response spectra of both horizontal components of

the ground-motion record. A unique scale factor is used for both components, which leads to inaccurate estimates of the median EDPs. The improved procedure, allowing for different scale factors for two horizontal components of ground motion, provides more accurate estimates of the median EDPs.

(3) The improved procedure results in more accurate and conservative results than those of the ASCE 7 procedure as the torsional irregularity increases. For buildings with highest irregularity factors for each plan type [for example, T05 ($\beta = 1.43$), L05 ($\beta = 1.35$) and R10 ($\beta = 1.13$)], the maximum discrepancies in story drift estimations of the original ASCE 7 procedure compared to the improved procedure were of −24% to +12%, −38% to +20%, and −31% to +19%, respectively ("−" indicates underestimation and "+" denotes overestimation of benchmark EDPs).

Nomenclature

The following symbols and abbreviations are used in this paper:

A_{mx}	median value of $SF_{1x} \cdot A_x$
A_{my}	median value of $SF_{1y} \cdot A_y$
$\hat{A}_x$	target pseudo-acceleration spectrum in x-direction
$\widehat{\mathbf{A}}_\mathbf{x}$	vector of spectral values $\hat{A}_x$
A_x	5%-damped response spectrum for x-component
$\mathbf{A}_\mathbf{x}$	vector of spectral values A_x
$\hat{A}_y$	target pseudo-acceleration spectra for y-direction
$\widehat{\mathbf{A}}_\mathbf{y}$	vector of spectral values $\hat{A}_y$
A_y	5%-damped response spectrum for y-component
$\mathbf{A}_\mathbf{y}$	vector of spectral values A_y
k	number of ground-motion records in a set
L	plan asymmetric about x- and y-axes
M	number of sets of k records
N	total number of vibration modes considered
R	quasi-rectangular plan
R_{JB}	Joyner–Boore distance
SF_x	final scale factor for x horizontal component of record
SF_y	final scale factor for y horizontal component of record
SF_{1x}	first scale factor for x horizontal component of record
SF_{1y}	first scale factor for y horizontal component of record
SF_{2x}	second scale factor for x horizontal component of record
SF_{2y}	second scale factor for y horizontal component of record
T	plan symmetric about y-axis
T_n	vibration period
x_{50}	median of a log-normal distribution
β	torsional irregularity factor
$\Delta_{\max}$	maximum story drift
$\Delta_{\mathrm{average}}$	average story drift
ε_x	maximum normalized difference for x horizontal component of record
ε_y	maximum normalized difference for y horizontal component of record
θ_p	plastic rotation
θ_y	yield rotation
μ	mean of a log-normal distribution
$\hat{\mu}$	geometric mean of a log-normal distribution

Acknowledgments

The authors would like to thank Charlie Kircher, Kishor Jaiswal, Brad Aagaard, Jamie Steidl, and three anonymous reviewers for their critical reviews, constructive comments, and editorial suggestions, which improved technical content and presentation of this paper.

Data and resources

Ground-motion records used in this study are available from the University of California, Berkeley Pacific Earthquake Engineering Research Center Ground-Motion Database at https://ngawest2.berkeley.edu/(last accessed on May 2018). The ground-motion selection and scaling procedure proposed herein are available as a MatLAB® function. This function and finite element models developed for this study are available from the authors upon request.

ORCID

Erol Kalkan http://orcid.org/0000-0002-9138-9407

References

Al-Atik, L. and Abrahamson, N. [2010] "An improved method for nonstationary spectral matching," *Earthquake Spectra* **26**(3), 601–617. doi:10.1193/1.3459159

Ambraseys, N., Douglas, J., Rinaldis, D., Berge-Thierry, C., Suhadolc, P., Costa, G., Sigbjörnsson, R. and Smit, P. [2003] *Dissemination of European Strong-Motion Data*, Vol. 2, CD-ROM Collection, Engineering and Physical Science Research Council, United Kingdom.

American Society of Civil Engineers [2010] "Minimum design loads for buildings and other structures," Report ASCE/SEI 7-10, Reston, VA.

American Society of Civil Engineers [2014] "Seismic evaluation and retrofit of existing buildings," Report ASCE/SEI 41-13, Reston, VA.

American Society of Civil Engineers [2016] "Minimum design loads for buildings and other structures," Report ASCE/SEI 7-16, Reston, VA.

Baker, J. [2011] "Conditional mean spectrum: tool for ground-motion selection," *Journal of Structural Engineering* **137**(3), 322–331. doi:10.1061/(ASCE)ST.1943-541X.0000215

Beyer, K. and Bommer, J. [2007] "Selection and scaling of real accelerograms for bi-directional loading: a review of current practice and code provisions," *Journal of Earthquake Engineering* **11**, 13–45. doi:10.1080/13632460701280013

Buratti, N., Stafford, P. and Bommer, J. [2011] "Earthquake accelerogram selection and scaling procedures for estimating the distribution of drift response," *Journal of Structural Engineering* **137**(3), 345–357. doi:10.1061/(ASCE)ST.1943-541X.0000217

Carballo, J. and Cornell, C. [1998] "Input to nonlinear structural analysis: modification of available accelerograms for different source and site characteristics," *Proceedings of the 6th U.S. National Conference on Earthquake Engineering*, Seattle, Washington.

Chadwell, C. B. and Imbsen, R. A. [2004] "XTRACT: A tool for axial force-ultimate curvature interactions," *Proceedings of the ASCE Structures Congress*, Nashville, Tennessee.

Computers and Structures Inc. [2006] *PERFORM 3D, User Guide V4, Non-Linear Analysis and Performance Assessment for 3D Structures*, Computers and Structures, Inc., Berkeley, CA.

Davison, A. C. [2009] "Statistical models," in *Cambridge Series in Statistical and Probabilistic Mathematics*, (Cambridge University Press, New York), pp. 726.

Han, S. and Seok, S. [2013] "Efficient procedure for selecting and scaling ground motions for response history analysis," *Journal of Structural Engineering* **140**(1). doi:10.1061/(ASCE)ST.1943-541X.0000881.

Hancock, J. [2006] "An improved method of matching response spectra of recorded earthquake ground motion using wavelets," *Journal of Earthquake Engineering* **10**, 67–89. doi:10.1080/13632460609350629

Hancock, J. and Bommer, J. [2007] "Using spectral matched records to explore the influence of strong-motion duration on inelastic structural response," *Soil Dynamics and Earthquake Engineering* **27**(4), 291–299. doi:10.1016/j.soildyn.2006.09.004

Haselton, C., Baker, J. W., Bozorgnia, Y., Goulet, C. A., Kalkan, E., Luco, N., Shantz, T., Shome, N., Stewart, J. P., Tothong, P., Watson-Lamprey, J. and Zareian, F. [2009] "Evaluation of ground motion selection and modification methods: predicting median interstory drift response of buildings," PEER Report No: 2009/01, Pacific Earthquake Engineering Research Center College of Engineering University of California, Berkeley, p. 219, June.

Haselton, C. B., Whittaker, A. S., Hortascu, A., Baker, J. W. and Grant, D. N. [2012] "Selecting and scaling earthquake ground motions for performing response-history analyses," *Proceedings of the 15th World Conference on Earthquake Engineering*, Lisboa, Portugal.

Huang, Y., Whittaker, A., Luco, N. and Hamburger, R. [2011] "Scaling earthquake ground motions for performance-based assessment of buildings," *Journal of Structural Engineering* **137**(3), 311–321. doi:10.1061/(ASCE)ST.1943-541X.0000155

International Code Council. [2010] *International Building Code*, IBC 2009, West Flossmoor Road, Country Club Hills, IL.

International Code Council. [2015] *International building code*, IBC 2015, West Flossmoor Road, Country Club Hills, IL.

International Code Council. [2016] *International Building Code*, IBC 2016, West Flossmoor Road, Country Club Hills, IL.

Jayaram, N. and Baker, J. [2008] "Statistical tests of the joint distribution of spectral acceleration values," *Bulletin of the Seismological Society of America* **98**(5), 2231–2243. doi:10.1785/0120070208

Jayaram, N., Lin, T. and Baker, J. W. [2011] "A computationally efficient ground-motion selection algorithm for matching a target response spectrum mean and variance," *Earthquake Spectra* **27**(3), 797–815. doi:10.1193/1.3608002

Kalkan, E. and Chopra, A. [2009] "Modal pushover-based ground motion scaling procedure for nonlinear response history analysis of structures," in *Proceedings of California Convention, Structural Engineers Association of California*, (San Diego, CA).

Kalkan, E. and Chopra, A. [2010] Practical guidelines to select and scale earthquake records for nonlinear response history analysis of structures, USGS Open-File Report 2010-1068, Menlo Park, CA, https://pubs.usgs.gov/of/2010/1068/.

Kalkan, E. and Chopra, A. [2011] "Modal-pushover-based ground-motion scaling procedure," *Journal of Structural Engineering* **137**(3), 298–310. doi:10.1061/(ASCE)ST.1943-541X.0000308

Kalkan, E. and Chopra, A. [2012] "Evaluation of modal pushover-based scaling of one component of ground motion: tall buildings," *Earthquake Spectra* **28**(4), 1469–1493. doi:10.1193/1.4000091

Kalkan, E. and Kwong, N. S. [2010] "Documentation for assessment of modal pushover-based scaling procedure for nonlinear response history analysis of 'ordinary standard' bridges," USGS Open-File Report 2010-1328:56, Menlo Park, CA, https://pubs.usgs.gov/of/2010/1328/.

Kalkan, E. and Kwong, N. S. [2012] "Assessment of modal pushover-based scaling procedure for nonlinear response history analysis of 'ordinary standard' bridges," *Journal of Bridge Engineering* **17**(2), 272–288. doi:10.1061/(ASCE)BE.1943-5592.0000259

Katsanos, E., Sextos, A. and Manolis, G. [2010] "Selection of earthquake ground motion records: a state-of-the-art review from a structural engineering perspective," *Soil Dynamics and Earthquake Engineering* **30**(4), 157–169. doi:10.1016/j.soildyn.2009.10.005

Kottke, A. and Rathje, E. M. [2008] "A semi-automated procedure for selecting and scaling recorded earthquake motions for dynamic analysis," *Earthquake Spectra* **24**(4), 911–932. doi:10.1193/1.2985772

Krawinkler, H. [1978] "Shear in beam-column joints in seismic design of frames," *Engineering Journal* **15**(3), 82–91.

Kwong, N. S. and Chopra, A. [2015] "Evaluation of the exact conditional spectrum and generalized conditional intensity measure methods for ground motion selection," *Earthquake Engineering and Structural Dynamics* **45**(5), 757–777. doi:10.1002/eqe.2683

Lilhanand, K. and Tseng, W. [1988] "Development and application of realistic earthquake time histories compatible with multiple-damping design spectra," *Proceedings of the 9th World Conference on Earthquake Engineering*, Tokyo-Kyoto, Vol. II, 819–824.

Mazza, F. and Labernarda, R. [2017] "Structural and non-structural intensity measures for the assessment of base-isolated structures subjected to pulse-like near-fault earthquakes," *Soil Dynamics and Earthquake Engineering* **96**, 115–127. doi:10.1016/j.soildyn.2017.02.013

O'Donnell, A. P., Kurama, Y. C., Kalkan, E., Taflanidis, A. A. and Beltsar, O. A. [2013] "Ground motion scaling methods for linear-elastic structures: an integrated experimental and analytical investigation," *Earthquake Engineering and Structural Dynamics* **42**(9), 1281–1300. doi:10.1002/eqe.2272

Reyes, J. and Chopra, A. [2012] "Modal pushover-based scaling of two components of ground motion records for nonlinear RHA of buildings," *Earthquake Spectra* **28**(3), 1243–1267. doi:10.1193/1.4000069

Reyes, J. and Kalkan, E. [2011] "Required number of ground motion records for ASCE/SEI-7 ground motion scaling procedure," U.S. Geological Survey Open-File Report No: 2011-1083, 34 p. https://pubs.usgs.gov/of/2011/1083/.

Reyes, J. and Kalkan, E. [2012] "How many records should be used in ASCE/SEI-7 ground motion scaling procedure," *Earthquake Spectra* **28**(3), 205–1222. doi:10.1193/1.4000066

Reyes, J. and Quintero, O. [2014] "Modal pushover-based scaling of earthquake records for non-linear analysis of single-story unsymmetric-plan buildings," *Earthquake Engineering and Structural Dynamics* **43**(7), 1005–1021. doi:10.1002/eqe.2384

Reyes, J., Riaño, A., Kalkan, E., Quintero, O. and Arango, C. [2014] "Assessment of spectrum matching procedure for nonlinear analysis of symmetric- and asymmetric-plan buildings," *Engineering Structures* **72**, 171–181. doi:10.1016/j.engstruct.2014.04.035

Reyes, J., Riaño, A., Kalkan, E. and Arango, C. [2015] "Extending modal pushover-based scaling procedure for nonlinear response history analysis of multi-story unsymmetric-plan buildings," *Engineering Structures* **88**, 125–137. doi:10.1016/j.engstruct.2015.01.041